EMPIRICAL ESTIMATION OF THE EFFECT OF URBAN HEAT ADVECTION ON THE TEMPERATURE SERIES OF DE BILT (THE NETHERLANDS)

T. BRANDSMA,* G. P. KÖNNEN and H. R. A. WESSELS

Royal Netherlands Meteorological Institute (KNMI), De Bilt, The Netherlands

ABSTRACT

The influence of urban heat advection on the temperature time series of the Dutch GCOS station De Bilt has been studied empirically by comparing the hourly meteorological observations (1993–2000) with those of the nearby (7.5 km) rural station at Soesterberg. Station De Bilt is in the transition zone (TZ) between the urban and rural area, being surrounded by three towns, Utrecht, De Bilt and Zeist. The dependence of the hourly temperature differences between De Bilt and Soesterberg on wind direction has been examined as a function of season, day- and night-time hours and cloud amount. Strong dependence on wind direction was apparent for clear nights, with the greatest effects (up to 1 °C on average) for wind coming from the towns. The magnitude of the effect decreased with increasing cloudiness. The analysis suggests that most of the structure in the wind direction dependence is caused by urban heat advection to the measuring site in De Bilt. The urban heat advection is studied in more detail with an additive statistical model. Because the urban areas around the site expanded in the past century, urban heat advection trends contaminate the long-term trends in the temperature series (1897–present) of De Bilt. Based on the present work, we estimate that this effect may have raised the annual mean temperatures of De Bilt by 0.10 ± 0.06 °C during the 20th century, being almost the full value of the present-day urban heat advection. The 0.10 ± 0.06 °C rise due to urban heat advection corresponds to about 10% of the observed temperature rise of about 1.0 °C in the last century. Copyright © 2003 Royal Meteorological Society.

KEY WORDS: temperature; urban heat advection; climate change; urban heat island; additive models; The Netherlands

1. INTRODUCTION

A factor that complicates the study of trends and long-term variability in global or regional temperatures is that, often, temperature stations contained in the world climate databases are located near growing urban areas. Even at some distance from urban centres, advection of the urban heat plume may be of sufficient strength to contaminate the long-term temperature variability of such stations. The importance of assessing and monitoring the magnitude of this effect is obvious.

There have been two major approaches to estimating the urban heat island (UHI) effect on temperature observations: bulk studies and single-station studies. In bulk studies, temperature series of a large number of stations are grouped together in a number of classes representing the degree of urbanization around the stations according to some particular criteria, after which the trends in the various classes are compared. From these bulk-type studies it has been concluded (Jones *et al.*, 1990; Easterling *et al.*, 1997; Folland *et al.*, 2001) that urban effects on globally and hemispherically averaged surface temperatures are relatively small at present (of order 0.05 °C for the period 1900 to 1990). However, on the regional scale the effect of urban warming might be much larger than on the global and hemispheric scale (Portman, 1993).

Single-station studies concentrate on the measurements of UHIs (the temperature difference between the urban area and the background rural area ΔT_{u-r}) for single cities as a function of meteorological conditions.

---

* Correspondence to: T. Brandsma, Royal Netherlands Meteorological Institute (KNMI), PO Box 201, 3730 AE De Bilt, The Netherlands; e-mail: theo.brandsma@knmi.nl

The most common approaches are: (1) to compare air temperature records inside a city with records of the adjacent rural area (e.g. Yagüe *et al.*, 1991; Karaca *et al.*, 1995; Magee *et al.*, 1999); and (2) to use data along transects obtained by using mobile units, like cars and trams (e.g. Moreno-Garcia, 1994; Yamashita, 1996; Montávez *et al.*, 2000). For the town of Utrecht, Conrads (1975) applied both approaches. In general, ΔT_{u-r} is found to be largest during nights with calm and clear conditions; its value under these conditions is denoted by $\Delta T_{u-r(max)}$. Factors like wind speed and cloudiness determine the relationship between ΔT_{u-r} and $\Delta T_{u-r(max)}$. Attempts have been made to relate $\Delta T_{u-r(max)}$ to non-meteorological factors like city population (Oke, 1973) and canyon geometry (Oke, 1981). These relationships indicate that for a city with 1 million inhabitants the $\Delta T_{u-r(max)}$ ranges between 8 (Europe) and 11 °C (North America) (Oke, 1973). Karl *et al.* (1988) extended this approach and derived equations for the USA that related ΔT_{u-r} to city population. These equations worked, however, only for the USA as a whole and not for individual US cities.

The extent to which urban heat is advected to measuring sites leeward is not known quantitatively. Away from cities, the mean UHI effect decreases rapidly. However, for certain combinations of UHI intensity and wind direction there may be a perceptible influence on temperature in the transition zone (TZ) between the urban and rural area (where the rural area is defined here as the area outside the sphere of influence of the city, not significantly influenced by the advection of urban warmth). On average, the temperature difference between the TZ and the rural area (ΔT_{TZ-r}) may be of the order of tenths of a degree celsius, which is small but important with respect to the climate signal in long-term temperature records. Although many temperature stations in the world climate databases are situated in TZs, much is still unknown on ΔT_{TZ-r}.

This paper studies the advection of urban heat to the measuring site of KNMI in De Bilt, which is situated in a TZ. For practical purposes, the temperature time series of De Bilt (1897–present) has always been used as a rural station, whereas it is actually one of those series suspected of being influenced by the surrounding urban areas. Therefore, the purpose of this paper may also be viewed as an attempt to answer the question of whether or not there is an urban bias in the long-term trend of this 'rural' site. The series has been used to monitor climate change in the Netherlands and is one used in the world databases of land-surface air temperature and in the GCOS surface network (Peterson *et al.*, 1997). For the present-day climate (1993–2000) we compare the hourly temperatures with those of the nearby rural station Soesterberg, yielding ΔT_{TZ-r}. The wind direction dependence of ΔT_{TZ-r} provides information on the relative importance of the advection of the urban heat in the temperature signal of the De Bilt record. The population statistics of the towns surrounding the station at De Bilt are used to obtain a first-order estimate of the 20th century contribution of urban heat advection on the De Bilt temperatures. We consider the present research as a first step to homogenize the De Bilt temperature series on a daily basis with respect to urban effects.

2. DATA AND METHODS

2.1. Study area

Figure 1 shows the location of the meteorological stations De Bilt (DB) and Soesterberg (SB) within the study area (rectangle) in the Netherlands. The distance between DB and SB is 7.5 km. In addition to SB, Figure 1 also shows the location of two other rural meteorological stations: Deelen (DL), 48 km east of DB; and Herwijnen (HW), 30 km south of DB. These stations are much further away from DB than SB and are used to examine the rural nature of SB.

Figure 2 shows a detailed (25 m resolution) land-use map of the study area. Land use is obtained from the national land cover data base LGN3 of the Netherlands, which is based on summertime satellite images of land use taken in the years 1995 and 1997 (de Wit *et al.*, 1999; Thunnissen and de Wit, 1999). There have been no significant changes in land use since then. The majority of the woods are coniferous. The figure shows that the measuring site DB is surrounded by three towns: De Bilt (33 000 inhabitants) extending from DB to the north, Utrecht (234 000 inhabitants) town border at about 2 km west and Zeist (60 000 inhabitants) town border at about 3 km southeast. Extending from DB, there is a forested area in directions between NNE and SE and mainly pasture in the other directions. In contrast to DB, the station SB has a much more rural
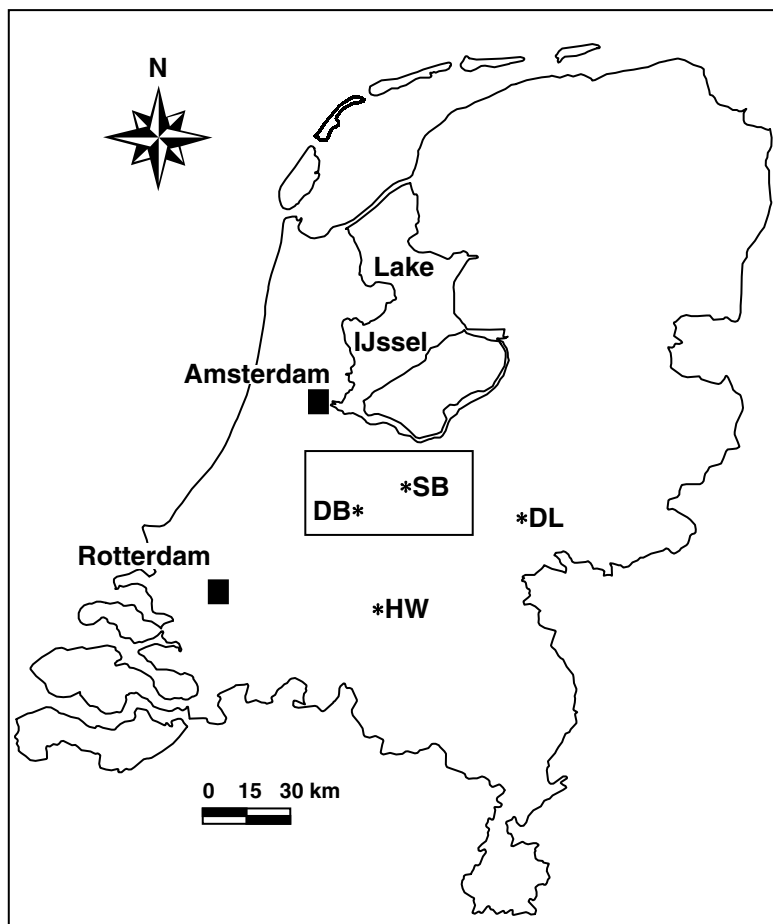
Figure 1. Location of study area (rectangle; see Figure 2) within the Netherlands, containing the meteorological station De Bilt (DB) in a transition zone (TZ) between urban and rural areas and the rural baseline station Soesterberg (SB). Also shown are the two alternative rural stations Deelen (DL) and Herwijnen (HW)

character. It is surrounded by a forested area and the only nearby town is Soesterberg (6000 inhabitants) situated just southeast of SB.

2.2. Station description and instrumentation

The four measuring sites DB, SB, DL and HW are all part of the national operational measuring network and have been set up and maintained according to the standards of the World Meteorological Organization. The measurements at all four sites are performed above short cut grass cover with standardized instruments and are sufficiently far removed from major obstacles. All sites are situated in relatively flat terrain. Figure 3 shows land use in 10×10 km^2 squares around each site. Table I presents some site-specific information.

For DB, the terrain roughness is large, especially for directions between southeast and north, where 15–30 m high trees are present at distances ranging between 80 to 220 m from the thermometer screen. At 30 m from DB, at 118°, there is an additional temperature screen, denoted DB* (screen, sensor and sampling frequency same as for DB). The measurements of this screen are available for the period 1995–2000.

SB is situated at the military airport of Soesterberg and is surrounded by forest. The minimum distance to the trees is about 300 m. There are two runways, one oriented northwest–southeast and one oriented west–east. The thermometer screen is situated in between the two runways. The northwest–southeast runway
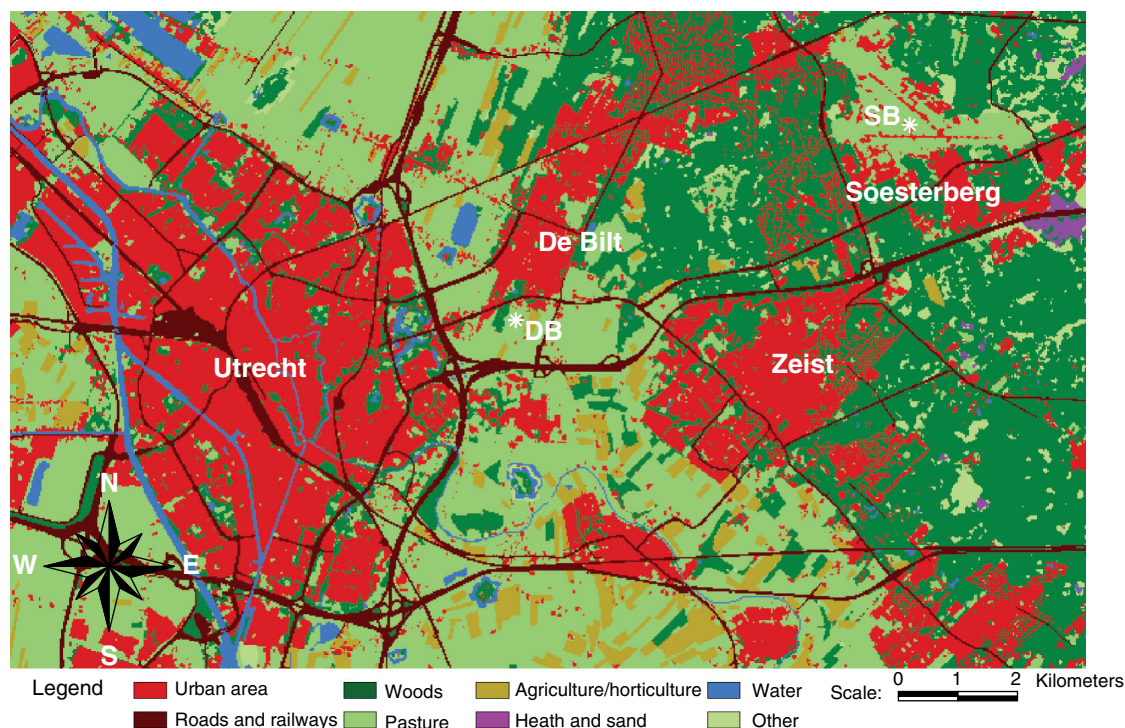
Figure 2. Detailed (25 m resolution) land-use map of the study area. Land use is obtained from the national land cover data base LGN3 of the Netherlands (see Section 2.1). The map covers an 18×11 km^2 area

is situated about 125 m northeast of the thermometer screen; the west–east runway is about 125 m south of the screen.

DL is situated at the military airport of Deelen in a forested area with pieces of heath land in between. In a northeasterly direction there is a row of 15–20 m high trees at about 85 m. The distance between the thermometer screen and the main runways is more than 500 m.

The site of HW is surrounded by pasture in all directions and there are no important obstacles for the airflow in the near vicinity.

Temperature at all four sites is measured at 1.5 m above ground level in naturally ventilated so-called KNMI multi-plate radiation shields (derived from Vaisala) using PT500 temperature sensors. The accuracy (accuracies always refer to the end of a calibration term) of the sensors is 0.1 °C (calibration term 36 months) and the resolution of the measurements is 0.01 °C. The hourly temperatures that have been used in this research are 1 min (DB and DB*) or 10 min averages (SB, DL, HW) centred at 10 min before the hour (UTC). Only the hourly wind data of DB have been used, and were measured on top of a pole at a height of 20 m. The pole is situated at a distance of about 230 m (at 100°) from the other instruments at DB. For wind direction, a wind vane has been used with an accuracy of 3° (calibration term 26 months) and a resolution of 1°. Wind speed has been measured with a cup-anemometer with an accuracy of 0.5 m/s (calibration term 26 months) and a resolution of 0.1 m/s. For hourly wind direction, 10 min averages have been used centred at 10 min before the hour (UTC) and for wind speed, 1 h averages have been used of the past hour (UTC). Like temperature, relative humidity is also measured in a naturally ventilated KNMI multi-plate radiation shield. The humidity sensor (Vaisala) has an accuracy of 3.5% (calibration term 8 months) and a resolution of 0.1%. The hourly humidity values that have been used are 1 min averages 10 min before the hour (UTC). Finally, the total fraction of cloud cover (in octas) has been observed by observers 10 min before each hour (UTC).
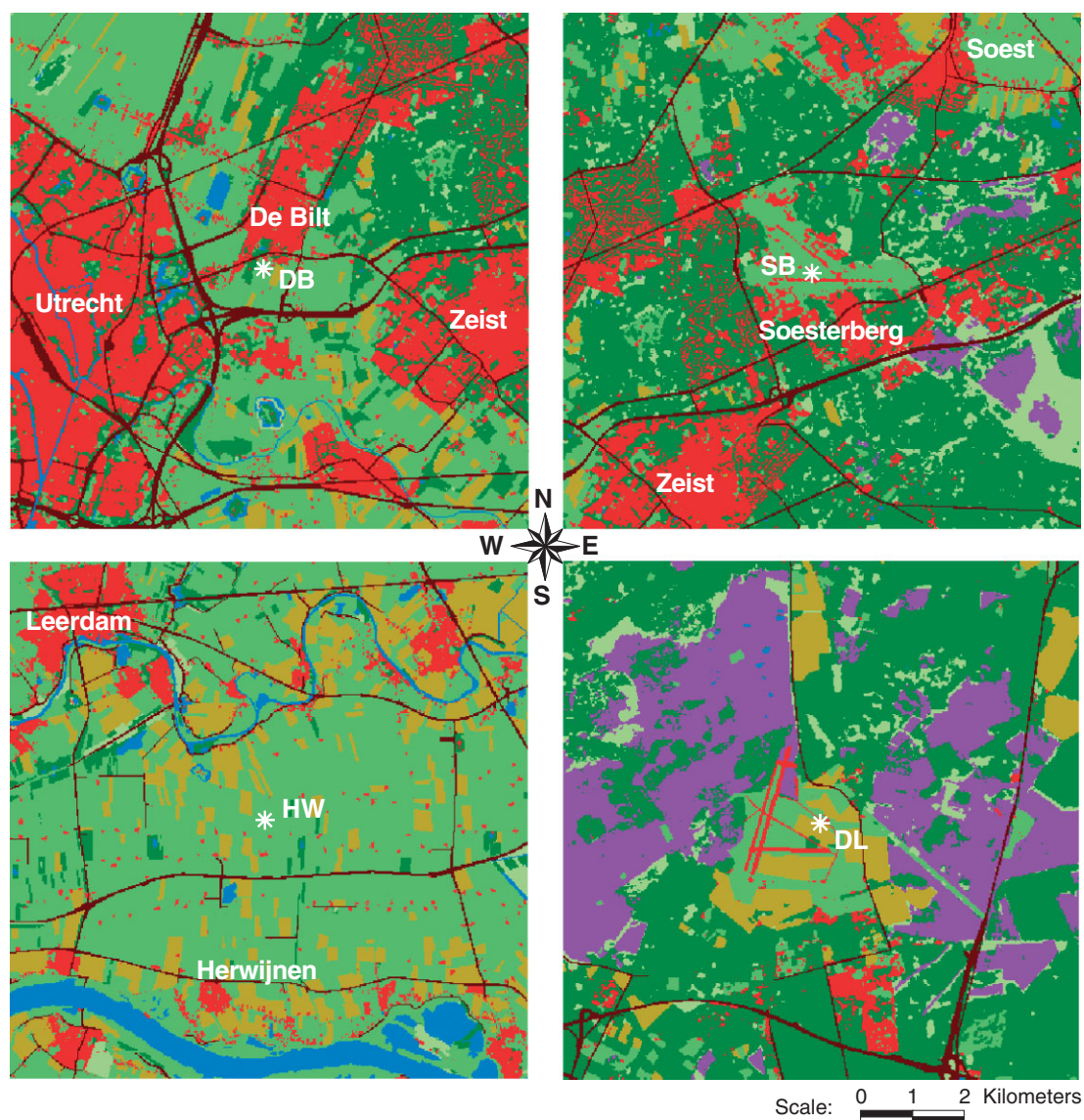
Figure 3. Detailed (25 m resolution) land-use map around all four sites: De Bilt (DB), Soesterberg (SB), DL (Deelen) and HW (Herwijnen). Land use is obtained from the national land cover data base LGN3 of the Netherlands (see Section 2.1). Each map covers a 10×10 km^2 area and has the site in its centre. Legend as Figure 2

2.3. Methodology

The advection of urban heat to the TZ-measuring site DB is studied by comparing the hourly temperature differences ΔT between DB and the rural reference station SB as a function of wind direction. The research is restricted to the period 1993–2000. Data before 1993 have not been included because of recorded changes in instrument type, shelter or position. The temperature differences are summarized for 36 wind direction classes (ranging between 10 and 360°) of 10° width. To account for a possible seasonal variation in ΔT_{u-r}, the night-time ΔT_{u-r} peak and the effects of stability on ΔT_{u-r}, we divided the data into two seasons (winter: October–March; summer: April–September); into daytime hours and night-time hours (according to the times of sunrise and sunset); and according to two cloud classes (hours with little cloud have an average degree of cloud cover $\leq 5/8$ and hours with greater cloud an average degree of cloud cover $>5/8$). This leads to

Table I. Site-specific information for the meteorological stations De Bilt (DB), Soesterberg (SB), Deelen (DL) and Herwijnen (HW)

Location	Lat (N)	Lon (E)	MSL[a] (m)	Soil type	GWL[b] (cm)	
					Summer	Winter
DB	52°06′	05°11′	2	Clay/sand	50–80	<40
SB	52°08′	05°17′	14	Sand	>160	>80
DL	52°04′	05°53′	47	Sand	>160	>80
HW	51°52′	05°09′	1	Clay	50–80	<40

[a] MSL: position of ground surface above mean sea level.
[b] GWL: groundwater level below ground surface.
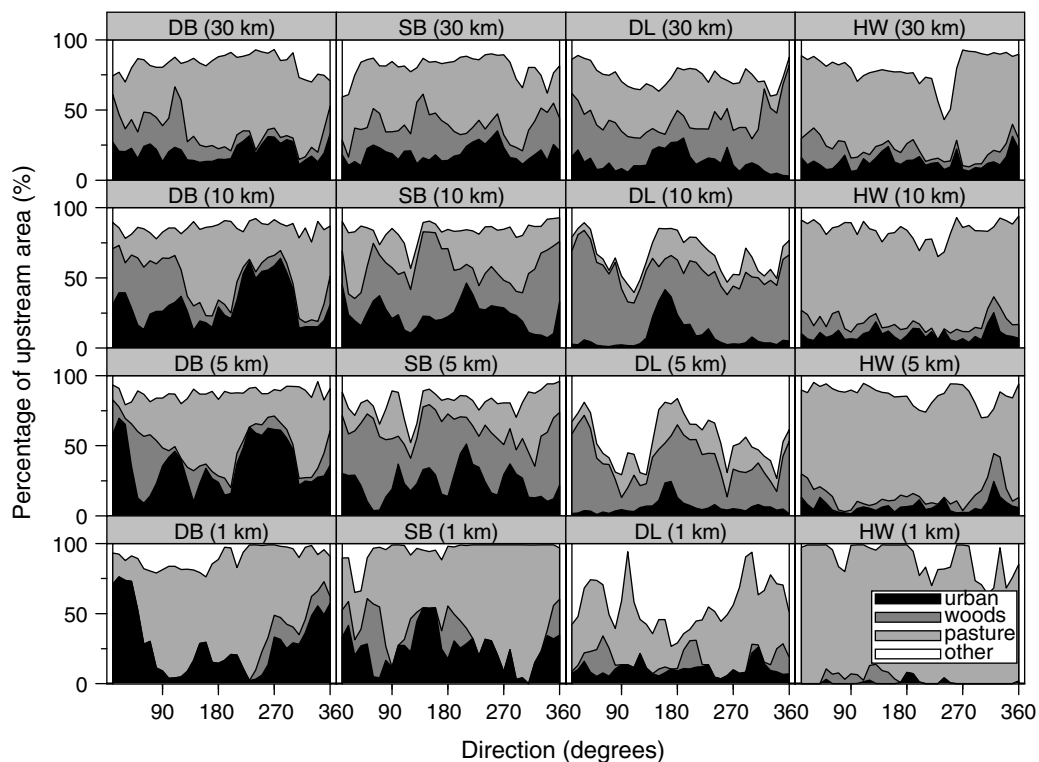
Figure 4. Percentage of upstream land use as a function of direction (10° resolution) for DB, SB, DL and HW for the three major land-use categories: urban, woods, pasture. Panels are shown for four values of the fetch: 1, 5, 10 and 30 km. For DL the large percentage of 'other' refers mainly to agriculture for a fetch of 1 km and to heath land for the larger values of the fetch. Land use is obtained from the national land cover data base LGN3 of the Netherlands (see Section 2.1)

eight categories in total. The meteorological situation, according to which the data were divided, refers to the observations at DB, not at the rural station. All hours where no wind direction could be recorded at DB (due to lack of wind) have not been taken into account.

For the study of advection of urban heat to a station, the characteristics of the area upstream of the station are of interest. Figure 4 shows the upwind average percentages of the three major land-use categories (urban, pasture, woods/heath) for DB, SB, DL and HW for four values of the fetch: 1, 5, 10 and 30 km. The figure evokes the question of whether Soesterberg is a good rural baseline station. This question will be addressed in Section 3.1, by mutually comparing DB, SB and the average of DL and HW (DL/HW). For the longest fetch

(30 km), Figure 4 shows urbanization more or less evenly distributed, for all stations and in all directions. This feature is characteristic for the Netherlands as a whole, and implies that there may be a background 'urban noise' that cannot be detected by wind-direction-dependent climatology of temperature differences between stations.

In Section 3.2, the relationship between vapour pressure differences (DB−SB) and temperature differences (DB−SB) is analysed using direction-dependent vapour pressure differences. In particular, during daytime conditions this measure may provide information about the relative coolness of upstream areas. This analysis is augmented by a discussion of the upstream soil dryness as derived from land use.

In Section 3.3, the dependence of the magnitude of advection of urban heat on various meteorological parameters is analysed in some more detail with an additive statistical model for wind coming from the direction of the most built-up areas: Utrecht and De Bilt.

In Section 3.4, the contribution of urban heat advection on the temperature series of DB for the current climate is estimated by determining a level on which urban heat advection peaks are supposed to be superimposed. In Section 3.5, the time dependence of this effect is studied using the population statistics of the towns surrounding DB to obtain a first-order estimate of the 20th century contribution of urban heat advection to the temperature trend of the DB time series.

3. RESULTS

3.1. Selection of a rural baseline for DB

To study the suitability of SB as a rural baseline station for DB, we defined the average of DL and HW (notated here as DL/HW) as an alternative rural baseline. Figure 4 shows that the rural nature of DL/HW is, in contrast to SB, undisputed. Figure 5 presents the mean monthly values of ΔT for DB−SB, DB−DL/HW and DL/HW−SB. The mean monthly values of ΔT for DB−SB and DB−DL/HW (left and middle panels) are $0.3\,°C$ and $0.4\,°C$ respectively, with maximum values in the winter half year. The night-time curve is always greater than the daytime curve up to about $0.3\,°C$, indicating a possible influence of urban heat advection to De Bilt. The pattern of DL/HW−SB (right panel) differs from the previous ones; in particular, for the
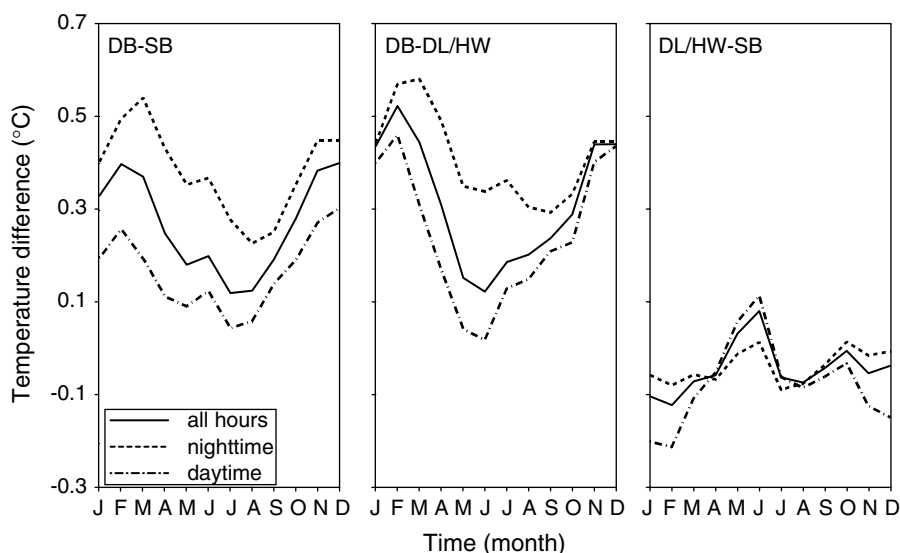
Figure 5. Mean monthly values of the temperature difference ΔT for De Bilt minus Soesterberg (DB−SB), De Bilt minus the average of Deelen and Herwijnen (DB−DL/HW) and the average of Deelen and Herwijnen minus Soesterberg (DL/HW−SB), for all hours, night-time hours and daytime hours for the period 1993–2000

night-time temperatures the annual variation is small (0.1 °C), with the largest values of the curves occurring in the month of June and the night-time curve is not always above the daytime curve.

Figures 6–8 show the wind direction dependence of ΔT in eight panels grouped according to season/day–night/cloudiness for DB–SB, DB–DL/HW and DL/HW–SB respectively. The similarity between Figures 6 and 7 is great. The upper panels in these figures show that, especially for nights with little cloud, ΔT is much larger (~0.4–1.2 °C) for wind coming from the town of Utrecht (270°) and De Bilt (20°) than for the other directions. During the day these peaks are hardly noticeable. In all cases, greater cloud cover weakens the peaks (lower panels of the figures). Compared with Figures 6 and 7, Figure 8 (DL/HW–SB) shows much less variation with wind direction. Although some panels in this latter figure show dependence on wind direction, e.g. on summer days with few clouds, the dependency on wind direction is small during the nights. We performed the same analysis by separating the dataset into (1) odd and even years and (2) the periods 1993–1996 and 1997–2000. In both cases, no conspicuous departures were noted from the results for the whole 1993–2000 period.

Although the above analysis indicates that both SB and DB/HW may be adequate rural baselines for DB, some details need to be discussed further. Firstly, the question arises as to how far the structures in Figures 6 and 7 are caused by local disturbances at the DB measuring site. To answer this question we compared DB with the parallel temperature screen DB* for the 1995–2000 period. For DB–DB* we produced figures (not shown) equal to Figures 6–8, but now also with a wind speed division: all wind speeds, wind speed ≤ 2 m/s and wind speed > 2 m/s. The analysis revealed no significant wind direction dependence in ΔT. For
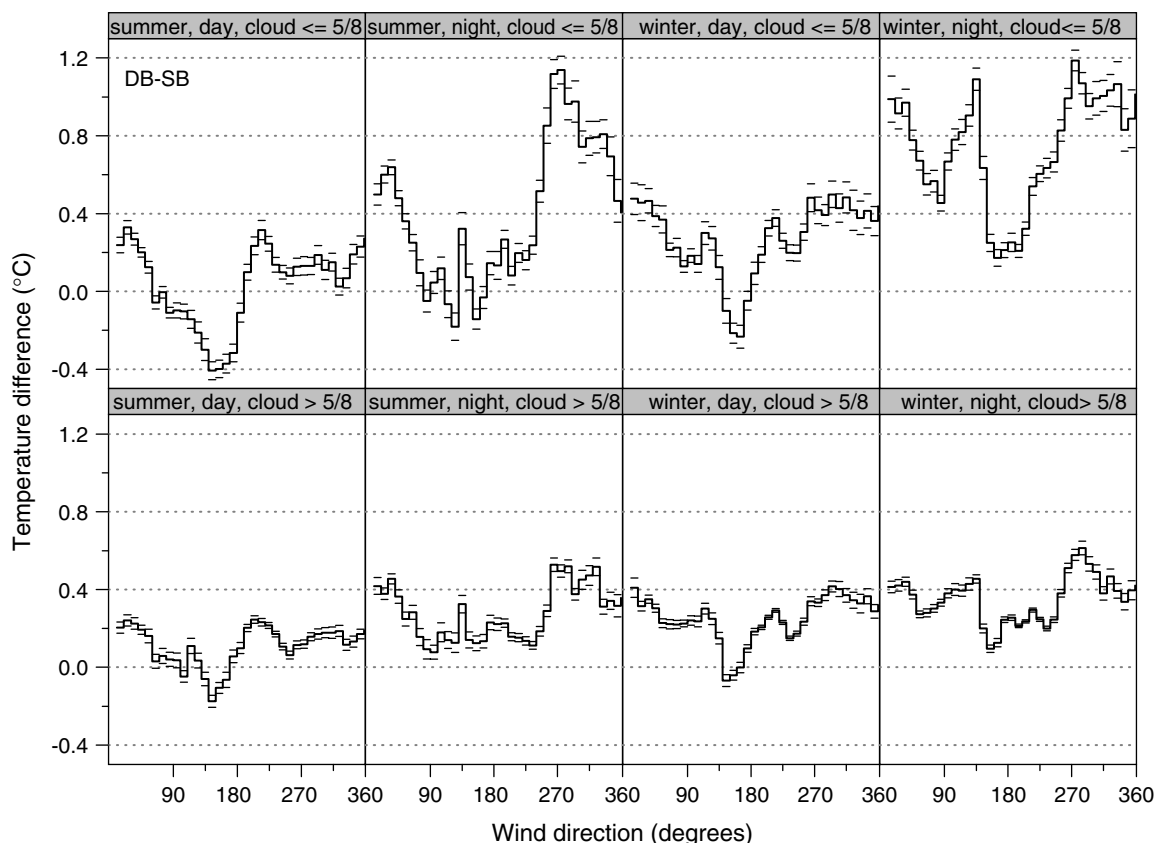
Figure 6. Dependence of temperature difference De Bilt minus Soesterberg (DB–SB) on wind direction: divided according to season, day- and night-time hours and cloud amount for the period 1993–2000 based on hourly observations. Upper panels have cloud cover ≤5/8; lower panels have cloud cover >5/8; left two panels are for summer (April–September) and right two panels for winter (October–March). The dashes give standard errors for each 10° wind direction class. See the text for definitions
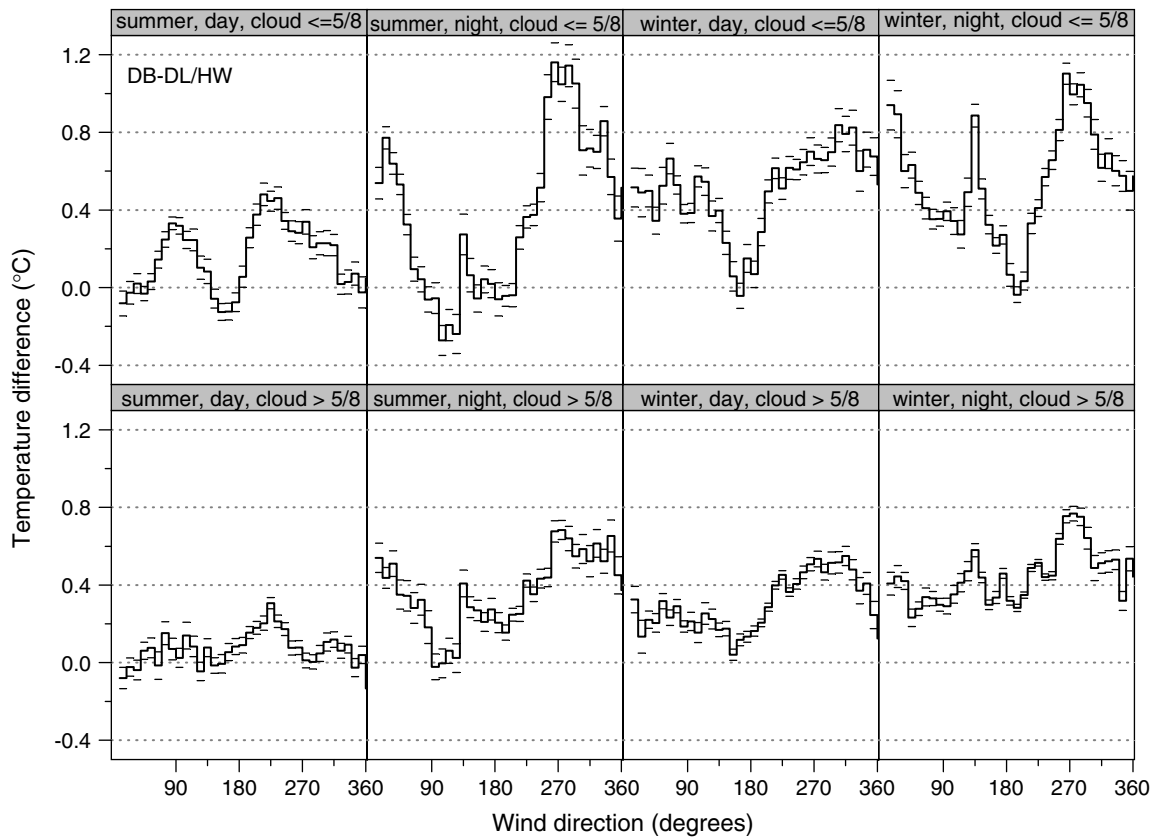
Figure 7. As Figure 6, but for De Bilt–Deelen/Herwijnen (DB–DL/HW)

wind speeds ≤ 2 m/s ΔT differed, in general, no more from the $\Delta T = 0\,°C$ line than the measuring accuracy (0.1 °C). For wind speeds >2 m/s we found a small dip in ΔT of about 0.2 °C for directions between 180 and 200° for both summer and winter nights with little cloud. This dip is probably related to the mutual position of DB and DB* with respect to a row of trees for those directions. From this we conclude that the structures in Figures 6 and 7 can be attributed to advection from larger distances than the measuring field at DB.

Secondly, in both Figures 6 and 7 there is a large narrow peak at 130° in summer and winter nights with little cloud (order 0.5 °C). This spike cannot reasonably be explained by Zeist, which is in the direction between 80 and 120°. We checked for the possibility of the existence of a strong point-energy source in the vicinity of DB in the 130° direction. Only a small power energy plant was found at about 1.2 km from DB in the 160° direction with its chimney at 45 m above MSL. Calculations on the distribution of the plume showed that its contribution to the spike is insignificant. Besides, the required wind shear (about 30–40°) between 45 m and screen level is too large to be realistic. An analysis of the wind direction dependence of ΔT for several wind speed classes (not shown) revealed that the 130° spike, in contrast to the peaks from the direction of Utrecht and De Bilt, disappeared for small wind speeds (≤ 2 m/s). For large wind speeds (>4 m/s) the peaks for the direction of Utrecht and De Bilt diminish and the 130° spike increases and becomes somewhat broader in decreasing direction. Consequently, we believe that the 130° spike has nothing to do with urban heat advection, but that it may be caused by either an unknown heat source or a large-scale effect related with the sharp transition from pasture to woods for the direction considered (see also Figure 4). However, attempts to decide between these two possibilities remained inconclusive.

Figure 6 shows for winter nights with little cloud cover an extension of the 130° spike to smaller angles. We attribute this feature, which is absent in Figure 7, to the presence of the Leusder Heide at about 110° from SB. The Leusder Heide is a piece of elevated heath land (5–6 km^2) with a large fraction of open sand
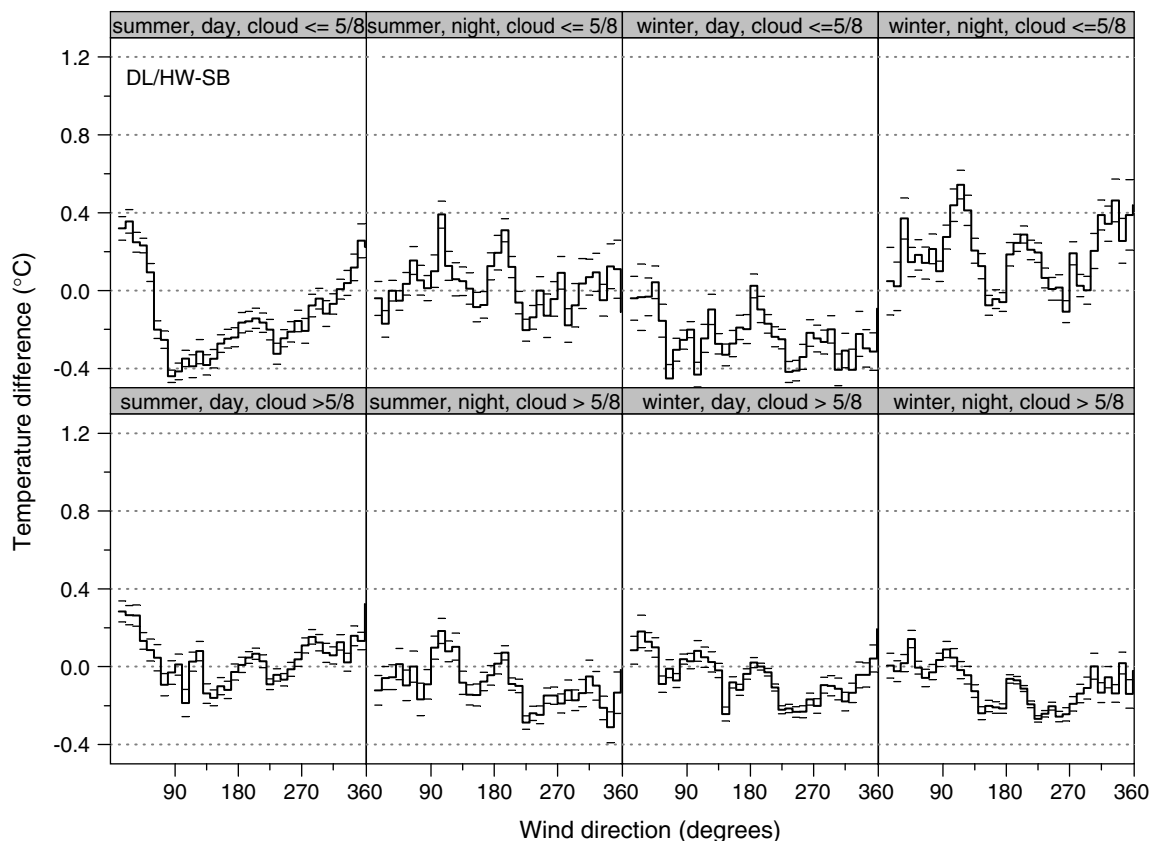
Figure 8. As Figure 6, but for Deelen/Herwijnen minus Soesterberg (DL/HW−SB)

area. Such a landscape may become cooler than the surroundings due to stronger radiative cooling during clear (winter) nights, causing a peak in the corresponding DB−SB panels.

Thirdly, both Figures 6 and 7 indicate a persistent dip with cloud cover ≤5/8 at 150° in the panels. The absence of such a structure in Figure 8 indicates that the dip is a feature related to DB. Apparently, this coolness is due to a terrain effect (differences in land use) that is unrelated to urbanization. This effect, among others, will be diagnosed further in Section 3.2. On summer days with northerly wind directions, both DB and SB are somewhat cooler than the DL/HW average, which may be related to the larger distance of the latter stations to Lake IJssel (Figure 1).

We conclude that, for the purpose of this study (to get a first-order estimate of the contribution of urban heat advection on the De Bilt temperatures), both SB and DL/HW are suitable to serve as a rural baseline for DB. We have, however, a slight preference for SB rather than for DL/HW. The main advantage of SB, compared with the DL/HW average, is that it is close to DB, resulting in the same degree of continentality as DB and the same distance to Lake IJssel. We believe this outweighs the disadvantage of SB of having a somewhat greater degree of upwind urbanization than DL/HW. Furthermore, the meteorological situation of DB correlates more closely with that of the nearby site SB than with DL/HW. For these reasons, the discussion will primarily focus on DB−SB rather than DB−DL/HW.

3.2. Analysis of vapour pressure differences and upstream soil dryness

Figure 9 shows the hourly vapour pressure differences Δe between DB and SB as a function of wind direction (same layout as Figures 6–8). Because humidity values are largest in summer, direction-dependent differences in Δe will also be largest in summer. Comparison of the daytime panels with those of Figure 6
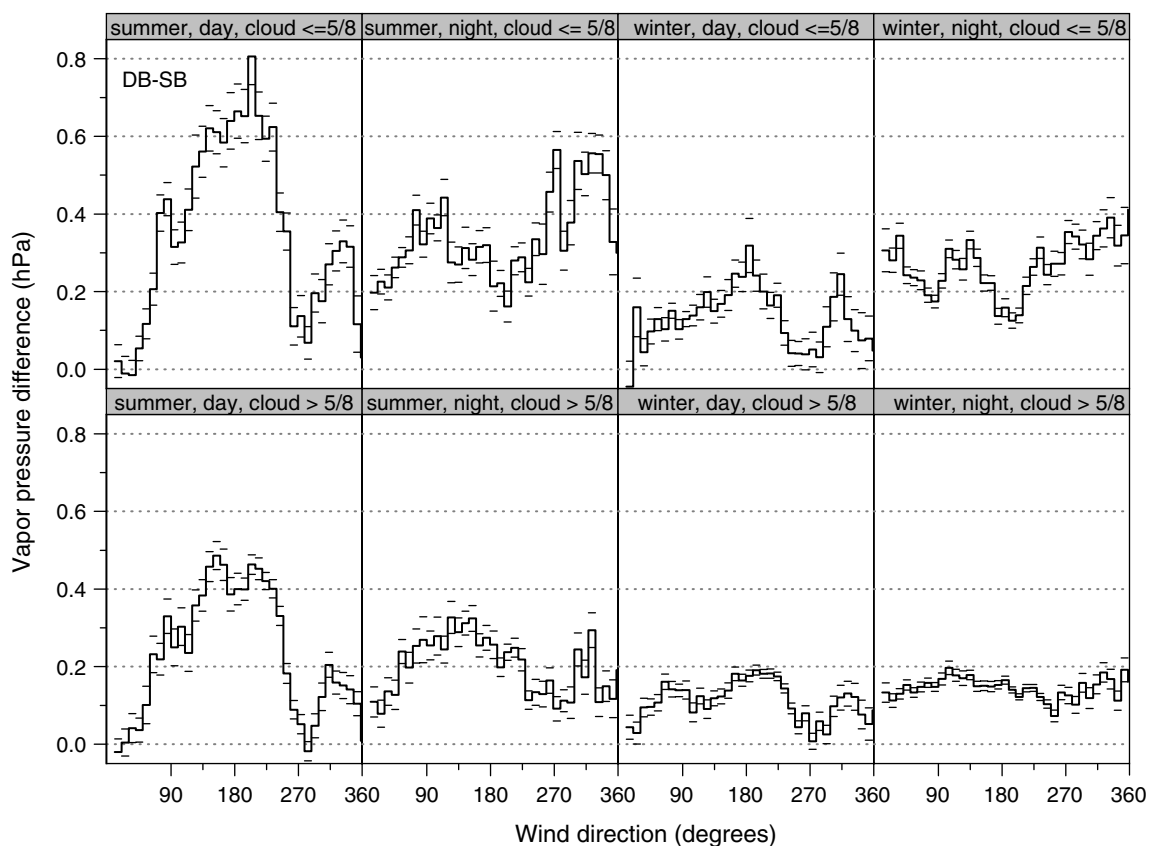
Figure 9. As Figure 6, but for the vapour pressure difference between De Bilt and Soesterberg (DB–SB)

shows that the Figure 9 peaks correspond roughly with dips in Figure 6. The peaks in vapour pressure are largest during summer days with few clouds. Large daytime values of Δe indicate that the air flowing to De Bilt passed over a surface that is relatively wet with respect to the other directions. As the latent heat flux is larger and the sensible heat flux smaller over a wet surface than over a dry surface, advection from wet surfaces will generally result in higher vapour pressures and lower air temperatures. At night, the heat fluxes are reversed and the excess values of the vapour pressure may result in dewfall, which involves the transformation of latent heat into sensible heat. The latter effect is, however, much smaller than the daytime effect, and thus hardly noticeable.

The effective radius of the area around a station that affects the vapour pressures at the stations is estimated by analysing the upstream soil dryness along the fetch as derived from land-use maps. Figure 10 shows a bulk measure of the upstream soil dryness as a function of direction, for fetches of 1, 5, 10 and 30 km, for DB, SB and DL/HW. We derived the dryness measure from the land-use categories in the LGN3 database (see Section 2.1). To do this, each land-use category was first ranked by us according to soil moisture class ranging between 0 (very wet) and 4 (very dry) (Wessels, 1983). Table II presents this ranking system for those land-use categories of interest for the present study, in which we note that irrigation in urban areas is, in general, insignificant in the Netherlands. In the next step, a weighted average of the ranking was calculated per degree along the fetches using a weighting function that decreased linearly (in 10 m intervals) from the stations of interest to the upper end of the fetch. Thereafter, we summarized the ranking into the 36 wind direction classes (ranging between 10 and 360°) of 10° width.

Figure 10 indicates that SB is relatively dry in most directions and for fetches up to 10 km, whereas the DL/HW average is relatively wet in all directions for all fetches. The upstream dryness DB shows a distinct structure. For fetches of 5 and 10 km there are maxima apparent in the directions of Utrecht and De Bilt and
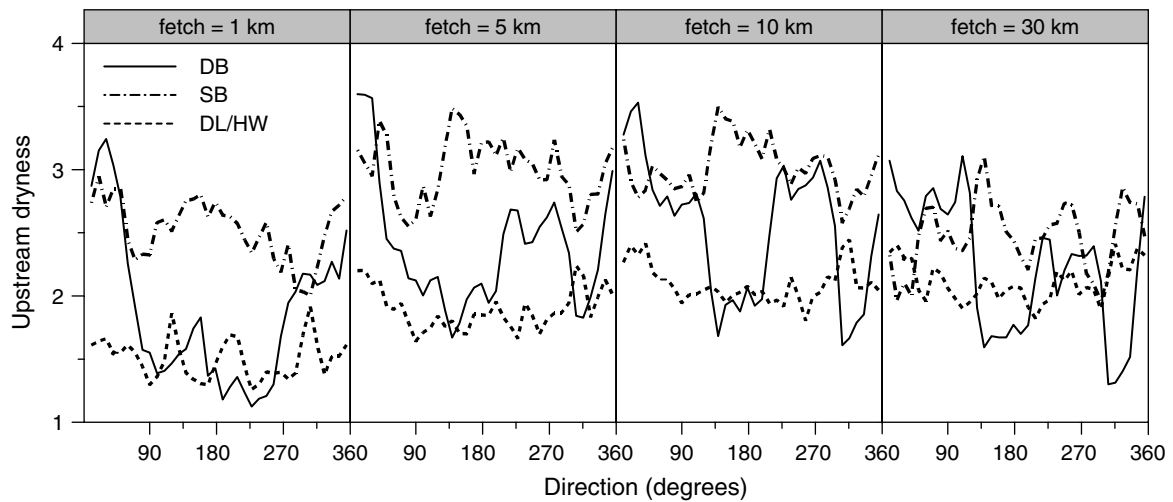
Figure 10. Upstream summertime dryness of the soil (derived from land-use classification, see text) as a function of direction (10° resolution) of DB, SB and the DL/HW average, for fetches of 1, 5, 10 and 30 km. The dryness scale runs from 0 (very wet) to 4 (very dry)

Table II. Ranking of land-use categories into soil moisture classes, ranging between 0 (very wet) and 4 (very dry)

Land use	Dryness	Land use	Dryness	Land use	Dryness
Surface waters	0	Grain	2	Coniferous wood in urban area	4
Pasture	1	Corn	2	Dry heath	4
Beet	1	Deciduous wood	2	Drifting sand	4
Deciduous wood in urban area	1	Heath	3	Built-up area	4
Pasture in urban area	2	Coniferous wood	4	Main roads and railways	4

minima in southeasterly and northwesterly directions. Note that the structure of DB dryness for fetches 1 and 5 km corresponds greatly with the structure in the night-time panels of Figure 6. The structure in the daytime panels in Figure 9 corresponds most closely with the structure of the difference between the upstream dryness of DB and SB in Figure 10 for fetches of 1 and 5 km in summer and for fetches of 5 and 10 km in winter. From this we conclude that the source area in winter is larger than in summer, which is probably related to the depth of the daytime planetary boundary layer, which is smaller in winter than in summer.

For the 5, 10, and 30 km fetches, the structure of the difference between the upstream dryness of DB and SB in Figure 10 shows minima around 150°, which correspond roughly with the daytime minima in Figure 6. From this, we conclude that the 150° dip in the temperature plot of DB−SB should be attributed mainly to upstream wetness of the soil.

3.3. Relative contributions in urban heat advection

To find the dependence of ΔT on cloudiness, wind speed and humidity for cases where urban heat advection is evident, we fitted an additive model for advection from Utrecht (wind direction between 210 and 300°) and advection from De Bilt (10−40°), both for night-time conditions. Additive models are defined by Hastie and Tibshirani (1990) as:

$$Y = \alpha + \sum_{j=1}^{p} f_j(X_j) + \varepsilon \tag{1}$$

where α is the intercept and Y and X_j are the predictant and predictors respectively. The errors ε are independent of the X_j values and $E(\varepsilon) = 0$ and $var(\varepsilon) = \sigma^2$. The functions f_j are arbitrary univariate (smooth) functions, one for each predictor. These models are particularly useful as analytic tools, as they allow non-linearity in the predictors. Since each variable is represented separately in Equation (1), the model retains an important interpretative feature of linear models: in the absence of interactions, the predictor effects can be analysed separately. Here, Equation (1) takes the following form:

$$\Delta T = \alpha + f_1(\text{cloudiness}) + f_2(\text{wind speed}) + f_3(\text{humidity}) + \varepsilon \tag{2}$$

where the functions f are smoothing splines (denoted as s in Figures 11 and 12) with four degrees of freedom. The average of each f equals zero.

Figures 11 and 12 show the fit of the model for advection from Utrecht to DB and De Bilt to DB respectively. The weighted average contribution of each variable in these plots is zero. All variables are significant at the 0.05 level. The standard errors in the figures are somewhat underestimated because the residuals of consecutive hours are serially correlated (lag-1 autocorrelation coefficient is ~0.5). The figures show that an increase in cloudiness and humidity results in a reduction of ΔT (thus decreasing the effect of urban heat advection on the DB temperatures). For wind speed the curves are different for summer and winter. The summertime curves suggest that, for urban heat advection to become most effective, some minimum wind speed >0.1 m/s (the lowest wind speed) is needed. For advection from Utrecht, the summertime curve shows a maximum at 2.2 m/s, whereas for advection from De Bilt the maximum is at 3.9 m/s. For larger wind speeds (>5 m/s) the effect of wind speed on urban heat advection decreases due to mixing of the heat plume with the overlying atmosphere. In contrast to the summertime curves, the wintertime curves in Figures 11 and 12 do not show a maximum. To investigate this further, we repeated the analysis for DB–DL/HW (not shown) and found maxima in both summer and winter wind-speed curves. We suggest that the absence of a
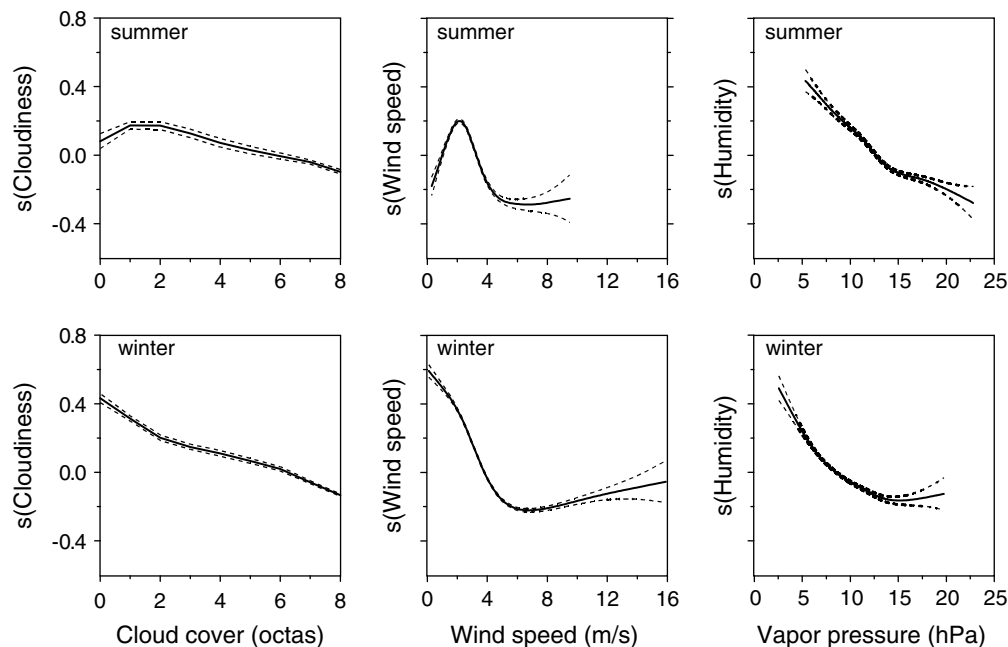
Figure 11. Smooth functions of the relative contribution of cloudiness, wind speed and humidity in the hourly temperature differences DB–SB (1993–2000) for the summer (upper panels) and winter half year (lower panels) for advection from Utrecht to DB (wind direction between 210 and 300°) during night-time hours. The functions s are smoothing splines with four degrees of freedom. The average contribution of each variable is set to zero. The dashed lines present the standard error values. The summer and winter panels use 3481 and 7554 data points respectively
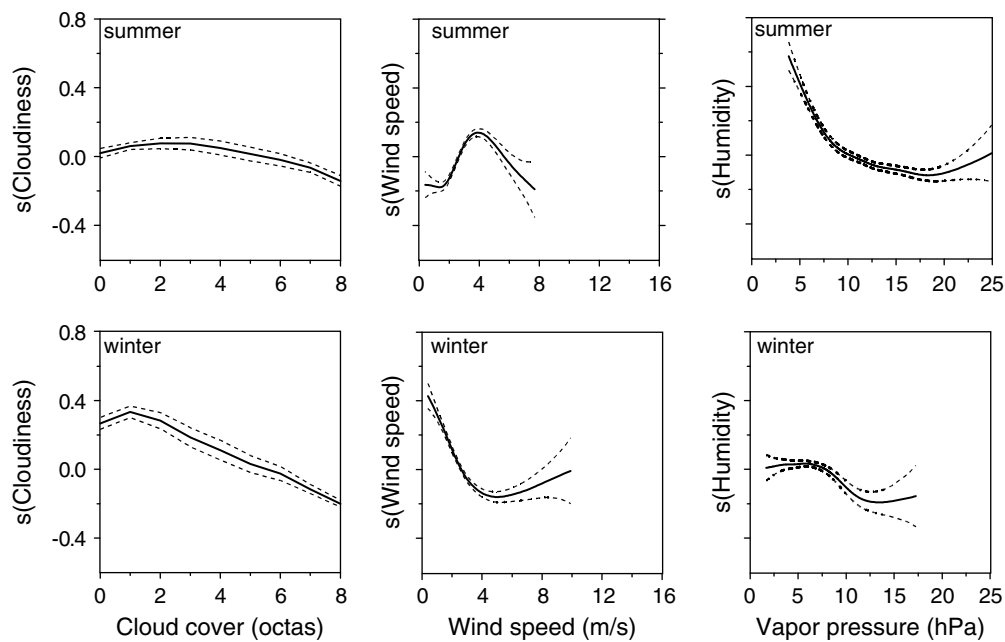
Figure 12. As Figure 11, but now for advection from De Bilt to DB (wind direction between 10 and 40°). The summer and winter panels use 1591 and 1085 data points respectively

maximum in the wintertime wind speed curves of Figures 11 and 12 is caused by local disturbances in air mass transformation at SB.

The assumption of no interaction between the predictors in Equation (2) is not completely justified. Further examination of interaction effects (not shown) reveals, for instance, that, for advection from Utrecht, the downward slope of the wind speed curve tends to become less steep with increasing cloudiness in both summer and winter. During summertime advection from Utrecht, the maximum in the wind-speed curve becomes smaller with increasing cloudiness, whereas for summertime advection from De Bilt the shape of the wind-speed curve depends strongly on humidity. The slopes of the cloudiness and humidity curves tend to become more horizontal with increasing wind speed. In summary, it should be realized that the curves in Figures 11 and 12 are average curves, and that the shape of the curve for one variable may vary more or less with the magnitude of the two other variables.

3.4. Estimate of the magnitude of urban heat advection for De Bilt

From Figure 6 (DB–SB), we estimated the contribution of urban heat advection (ΔT_{adv}) for the 1993–2000 period in the temperature series of De Bilt as follows. For each panel in Figure 6 we determined a level δ on which urban heat advection peaks were supposed to be superimposed. The value of δ was found from the wind directions with advection from the rural areas, neglecting the dip at about 150°, which is found to be the result of direction-dependent upstream soil wetness differences (Section 3.2). Values in a plot $>\delta$ were assumed to be caused by urban heat advection. As shown in Section 3.1, the spike at 130° is unrelated to urban heat advection and the values between 80 and 120° cannot be fully explained by Zeist. To compensate for this, ΔT_{adv} values for the 120 and 130° wind direction classes were set to zero. The mean effect of ΔT_{adv} on the annual temperature of DB was found by first calculating the wind direction weighted-mean ΔT_{adv} for each panel, and then the cloud and day-length weighted mean over all eight panels. To account for the uncertainty in the determination of δ, the calculations were repeated for $\delta + 0.1$ and $\delta - 0.1$.

The results are presented in Table III, which demonstrates that the contribution of large peaks in Figure 6 to the overall ΔT_{adv} is, in the case of DB, relatively small. For instance, the contribution of the large peak

Table III. Estimated contribution of the present-day urban heat advection ΔT_{adv} to the mean temperature for each panel in Figure 6 for three thresholds. δ is the estimated value in the Figure 6 panels on which the urban heat advection peaks are superimposed. The last two columns give the results for $\delta - 0.1\,°C$ and $\delta + 0.1\,°C$. The lower row gives the weighted mean of ΔT_{adv} for the year temperatures. Data are for 1993–2000

Panel	Hours	δ (°C)	$\Delta T_{adv}(\delta)$ (°C)	$\Delta T_{adv}(\delta - 0.1)$ (°C)	$\Delta T_{adv}(\delta + 0.1)$ (°C)
Summer, day, cloud $\leqslant$5/8	7604	0.0	0.11	0.19	0.05
Summer, night, cloud $\leqslant$5/8	5564	0.1	0.28	0.36	0.22
Winter, day, cloud $\leqslant$5/8	3544	0.2	0.10	0.17	0.05
Winter, night, cloud $\leqslant$5/8	6870	0.5	0.20	0.27	0.14
Summer, day, cloud >5/8	12 819	0.1	0.06	0.14	0.01
Summer, night, >5/8	6013	0.2	0.09	0.16	0.05
Winter, day, >5/8	9630	0.2	0.06	0.13	0.01
Winter, night, >5/8	12 937	0.2	0.10	0.19	0.05
Weighted mean			0.11	0.19	0.06

for westerly flow during summer nights with few clouds (second panel from the left of the upper panels in Figure 6) is weakened, because (1) there are only 8% of summer nights with few clouds, and (2) in such summer nights the prevailing wind direction is northeast; only 16.0% of the time does the wind blow from the sector southwest–northwest. The lower row in Table III shows that the overall ΔT_{adv} ranges between 0.06 and 0.19 °C, with a central estimate of 0.11 °C, for the values of δ considered. The difference between the overall ΔT_{adv} for summer and winter is negligible (not shown). For comparison purposes, we repeated the analysis using DL/HW instead of SB as a baseline (with slightly different values of δ). In that case the overall ΔT_{adv} ranges between 0.08 and 0.21 °C, with a central estimate of 0.14 °C.

3.5. Time dependence of urban heat advection to De Bilt

The meteorological station DB was set up in 1897. Because of the expansion of the towns of Utrecht, De Bilt and Zeist, it is plausible that part of the $0.11 \pm 0.06\,°C$ advected urban heat to De Bilt was time dependent since 1897. Here, we attempt to obtain a rough estimate of the time dependency.

In general, expansion of towns will affect the urban heat advection to stations in the TZ in three ways: (1) it enlarges the wind direction sector for which urban heat is advected; (2) it increases ΔT_{u-r}; and (3) it reduces the distance of the station to the town border. Here, we concentrate on the first two of these influences only.

To estimate the contribution of urban heat advection ΔT_{adv} at the end of the 19th century relative to the present-day values, we make three simplifications. First, we assume that the shapes of the towns (Utrecht, De Bilt and Zeist) have always been circular. This implies that the town diameter D is proportional to the square root of the town area A. Second, we assume that ΔT_{adv} is proportional to D. This takes into account the larger wind direction sector for which urban heat is advected in the case of town expansion. And third, we assume that ΔT_{adv} is proportional to the average value of ΔT_{u-r} over all meteorological conditions, denoted as $\overline{\Delta T}_{u-r}$. This value $\overline{\Delta T}_{u-r}$ is anticipated to be a better indicator of ΔT_{adv} than $\Delta T_{u-r(max)}$. The value of $\overline{\Delta T}_{u-r}$ is about proportional to the square root of city population P (Karl *et al.*, 1988), whereas $\Delta T_{u-r(max)}$ is related to the logarithm of P (Oke, 1973). Although the latter result was obtained for American cities, we assume that it can be applied to the European situation, too. In both cases, P has been used as a surrogate for city area A.

From the information above it can be deduced that $\Delta T_{adv} \propto \sqrt{A}\sqrt{A} = A$. From a census in 1899 we know that the town of Utrecht then contained 102 000 inhabitants (44% of present), the town of De Bilt 3000 inhabitants (9% of present) and the town of Zeist 8700 inhabitants (15% of present). Because the number of persons per household decreased by about a factor of two in the 20th century, the surface area of the three towns around the year 1899, compared with the present surface area, equals about 22.0% for Utrecht, 4.5% for De Bilt and 7.5% for Zeist. For Utrecht, this means that ΔT_{adv} in 1899 equals 22% of the present-day value,

for De Bilt 4.5% and for Zeist 7.5%. The overall ΔT_{adv} in 1899 can now be calculated as a weighted average of these values. Assuming weights of 0.5 for Utrecht, 0.3 for De Bilt and 0.2 for Zeist, ΔT_{adv} in 1899 equals 13.8% of the present-day value. Using the results in Section 3.4, we now estimate that $0.10 \pm 0.06\,°C$ of the 20th century warming trend of $1.0\,°C$ (which we calculated from the 20th century temperature data of DB) in the DB series should be attributed to (intensifying) urban effects rather than to changes in local/regional climate. Note that this value of $0.10 \pm 0.06\,°C$ represents almost the full value of the present-day urban heat advection (Table III). When we use DL/HW as a baseline instead of SB the estimate is slightly greater and equals $0.12 \pm 0.06\,°C$.

4. DISCUSSION AND CONCLUSIONS

We explored the potential of wind-direction-dependent hourly temperature climatology for determining the influence of urban heat advection on a long-term temperature record. The method relies on the ability to find a good baseline station. In the case of DB, the temperature series of the nearby rural station SB could be used as a satisfactory baseline station. The conjecture that DB is not a rural station but a station in a TZ was proved by independent comparisons of DB with SB and DL/HW. Although the method is able to demonstrate the advection of urban heat to DB and to provide an estimate of the maximum of the effective distance of the order of several kilometres, a precise assessment of the magnitude of the effect is complicated by inhomogeneities in the distribution of land use and soil moisture on scales up to 10 km or more. On the smaller scale (1 cm–1 km), differences in, for instance, the direction-dependent surface roughness may have an effect, as well as the situation of buildings and, for the case of SB, runways. The effects of all these factors are difficult to assess. Nevertheless, we were able to obtain an estimate of the contribution of urban heat advection to the mean temperatures in De Bilt. For the 20th century, the effect of increased urbanization on temperature was estimated as $0.10 \pm 0.06\,°C$ (comparison with the alternative baseline DL/HW yields $0.13 \pm 0.06\,°C$). This value is somewhat larger than the global and hemispheric average value of $0.05\,°C$ (Jones *et al.*, 1990; Easterling *et al.*, 1997) over the period 1900 to 1990. As expected, DB is more than an average station influenced by the surrounding urban areas.

Urban heat advection to DB may also originate from larger distances, for instance from the two largest cities of the Netherlands: Amsterdam (35 km northwest of DB) and Rotterdam (46 km southwest of DB). For such scales, Best and Clark (2002) demonstrated for the area around London that the urban heat may be transported tens of kilometres downwind of the city. However, comparison of DB and SB with the DL/HW series does not reveal an effect of Amsterdam and Rotterdam, despite the fact that the situation of DL and HW with respect to Amsterdam and Rotterdam differs from that of DB and SB. From this we infer that the effect of long-distance advection of urban heat to DB is probably small compared with the advection from Utrecht and De Bilt. However, more research is needed to obtain firm conclusions on long-distance urban heat advection.

In order, systematically, to homogenize long-term daily to hourly temperature time series to account for the effect of urban heat advection, some more work needs to be done. As for most long temperature time series, there will not be an accompanying hourly baseline station for the same long period. Therefore, it may be worthwhile examining to what extent a long-term stand-alone hourly (or daily maximum and minimum) temperature series can be used, in combination with wind direction and possibly cloudiness, to separate the contribution of urban heat advection. For instance, the wind-direction dependence for night-time hours may be compared with that of the daytime hours as a function of time. Much is also to be expected from studies with high-resolution mesoscale models, like that of Best and Clark (2002). However, for DB, those studies will have to wait until resolutions of hundreds of metres are available in these models. Finally, on the global or hemispheric scale, it may be of interest to perform bulk-type studies with daily temperature and wind direction data, taking into account the position of stations compared with the urban areas.

REFERENCES

Best MJ, Clark PA. 2002. The influence of vegetation on urban climate. In *Fourth Symposium on the Urban Environment, 20–24 May 2002, Norfolk, Virginia*. American Meteorological Society: Boston.

Conrads LA. 1975. *Observations of meteorological urban effects. The heat island of Utrecht.* PhD thesis, University of Utrecht, Utrecht.

De Wit AJW, van der Heijden ThGC, Thunnissen HAM. 1999. Vervaardiging en nauwkeurigheid van het LGN3 grondgebruiksbestand. Wageningen, DLO-Staring Centrum. Report 663 (in Dutch).

Easterling DR, Horton B, Jones PD, Peterson TC, Karl TR, Parker DE, Salinger MJ, Razuvayev V, Plummer N, Jamason P, Folland CK. 1997. Maximum and minimum temperature trends for the globe. *Science* **277**: 364–367.

Folland CK, Karl TR, Christy JR, Clarke RA, Gruza GV, Jouzel J, Mann ME, Oerlemans J, Salinger MJ, Wang S-W. 2001. Observed climate variability and change. In *Climate Change 2001: The Scientific Basis. Contribution of Working Group I to the Third Assessment Report of the Intergovernmental Panel on Climate Change*, Houghton JT, Ding Y, Griggs DJ, Noguer M, van der Linden PJ, Dai X, Maskell K, Johnson CA (eds). Cambridge University Press: Cambridge, UK and New York, NY, USA.

Hastie TJ, Tibshirani RJ. 1990. *Generalized Additive Models.* Monographs on Statistics and Applied Probability 43. Chapman and Hall: London.

Jones PD, Groisman YaP, Coughlan M, Plummer N, Wang W-C, Karl TR. 1990. Assessment of urbanization effects in time series of surface air temperature over land. *Nature* **347**: 169–172.

Karaca M, Tayanç M, Toros H. 1995. Effects of urbanization on climate of Istanbul and Ankara. *Atmospheric Environment* **29**: 3411–3421.

Karl TR, Diaz HF, Kukla G. 1988. Urbanization: its detection and effect in the United States climate record. *Journal of Climate* **1**: 1099–1123.

Magee N, Curtis J, Wendler G. 1999. The urban heat island effect at Fairbanks, Alaska. *Theoretical and Applied Climatology* **64**: 39–47.

Montávez JP, Rodríguez A, Jiménez JI. 2000. A study of the urban heat island of Granada. *International Journal of Climatology* **20**: 899–911.

Moreno-Garcia MC. 1994. Intensity and form of the urban heat island in Barcelona. *International Journal of Climatology* **14**: 705–710.

Oke TR. 1973. City size and the urban heat island. *Atmospheric Environment* **7**: 769–779.

Oke TR. 1981. Canyon geometry and the nocturnal urban heat island: comparison of scale model and field observations. *Journal of Climatology* **1**: 237–254.

Peterson TC, Daan H, Jones PD. 1997. Initial selection of a GCOS surface network. *Bulletin of the American Meteorological Society* **78**: 2145–2152.

Portman DA. 1993. Identifying and correcting urban bias in regional time series: surface temperature in China's northern plains. *Journal of Climate* **6**: 2298–2308.

Thunnissen HAM, de Wit AJW. 1999. The national land cover database of the Netherlands. In *Geoinformation For All; XIX Congress of the International Society for Photogrammetry and Remote Sensing (ISPRS)*, Beek KJ, Molenaar M (eds). International Archive of Photogrammetry and Remote Sensing, vol. 33, part B7/3. GITC: 2000; 223–230 (cd-rom).

Wessels HRA. 1983. A soil moisture map of the Netherlands for studies of atmospheric convection. KNMI Memorandum FM-83-28, De Bilt.

Yagüe C, Zurita E, Martinez A. 1991. Statistical analysis of the Madrid urban heat island. *Atmospheric Environment B* **25**: 327–332.

Yamashita S. 1996. Detailed structure of heat island phenomena from moving observations from electric tram-cars in metropolitan Tokyo. *Atmospheric Environment* **30**: 429–435.